ELSEVIER

Biochimica et Biophysica Acta 1368 (1998) 41–51

BIOCHIMICA ET BIOPHYSICA ACTA
BBA

Catalytic hydrogenation of polyunsaturated biological membranes: effects on membrane fatty acid composition and physical properties

James A. Logue [a,*], László Vigh [b], Ferenc Joó [c], Andrew R. Cossins [a]

[a] *School of Biological Sciences, University of Liverpool, Liverpool L69 3BX, UK*
[b] *Institute of Biochemistry, Biological Research Centre, Hungarian Academy of Sciences, H-6701 Szeged, Hungary*
[c] *Institute of Physical Chemistry, Kossuth Lajos University, H-4010 Debrecen, Hungary*

Received 20 March 1997; revised 8 July 1997; accepted 18 August 1997

Abstract

The relationship between phospholipid saturation and membrane physical structure in a complex, highly polyunsaturated biological membrane (trout liver microsomes) has been studied by the graded and specific hydrogenation of polyunsaturated fatty acids. The homogeneous catalyst $Pd(QS)_2$ caused rapid and effective hydrogenation, increasing the proportion of saturated fatty acids from 20–30% up to 60%, without loss or fragmentation. Long chain, polyunsaturated fatty acids (20:5ω3, 22:6ω3) were rapidly converted to a large number of partially hydrogenated isomers, and ultimately to the fully saturated C20 or C22 fatty acids. C18 mono- and di-unsaturates showed slower rates of hydrogenation. Increased saturation was closely associated with an increased membrane physical order as determined by the fluorescence anisotropy probe, 1,6-diphenyl-1,3,5-hexatriene. However, extensive hydrogenation led to highly ordered membranes exhibiting a gel-liquid crystalline phase transition between 30 and 60°C. Polyunsaturated membranes can thus be converted into partially or substantially saturated membranes with measurable phase structure without direct alteration of other membrane components. This offers a less equivocal means of assessing the influence of polyunsaturation upon membrane structure and function.

Keywords: Catalytic hydrogenation; Lipid hydrogenation; Membrane fluidity; Fatty acid saturation; Polyunsaturated fatty acid; Fish membrane

1. Introduction

Biological membranes are composed of phospholipids containing mixtures of saturated and unsaturated fatty acids. The phase structure and degree of molecular disorder of these membranes is heavily dependent upon the exact balance of fatty acids, with unsaturation generally causing hydrocarbon disorder by the steric hindrance of attractive lipid–lipid interactions [1]. This knowledge has been built up largely using model membranes composed of simple lipid mixtures. Biological membranes are composed of more complex mixtures, especially in higher animals and plants, yet comparatively little effort has gone into understanding how this complexity relates to structural and functional properties of these membranes. In particular, the extensive polyunsaturation

Abbreviations: DPH, 1,6-diphenyl-1,3,5-hexatriene; PC, phosphatidylcholine; PE, phosphatidylethanolamine; PUFA, polyunsaturated fatty acid; $Pd(QS)_2$, palladium di(sodium alizarinmonosulfonate)

* Corresponding author. Fax: +44 151 794 5094; E-mail: j.a.logue@liverpool.ac.uk

0005-2736/98/$19.00
PII S0005-2736(97)00203-4

of membrane fatty acids seen in animal membranes lacks an adequate explanation. Studies of polyunsaturated fatty acids in model membranes have suggested that physical structure is influenced more by the proportion of unsaturated fatty acids than by the degree of unsaturation of the unsaturated fatty acids.

Several methods have been employed to alter fatty acid saturation, including the manipulation of fatty acid biosynthesis, membrane delipidation and reconstitution experiments and dietary supplementation. However, with all of these methods, it is not possible to exclude contributions from an altered protein complement or composition, altered lipid-headgroup distribution and other aspects of membrane composition. Recent approaches to the regulation of gene transcription in response to altered membrane physical structure requires an ability to manipulate bilayer structure and lipid saturation without altering other components [2,3].

One direct method of manipulating lipid saturation without affecting other membrane components is the direct in situ chemical hydrogenation of unsaturated membrane fatty acids using catalysts. $Pd(QS)_2$, the palladium (II) complex of sodium alizarine monosulphonate [4], has been used to hydrogenate model membranes [5], microsomes [6], isolated organelles [7] and the membranes of isolated living cells [8,9]. It is highly substrate specific since hydrogenation of chloroplasts proceeds with the reduction of C=C bonds in membrane fatty acids but not in the neutral lipid chlorophylls, carotenoids and plastoquinones [10]. Oxo acids such as pyruvate are also not hydrogenated and there are no reports concerning saturation of double bonds of other non-lipid compounds.

Biological studies with the homogeneous catalyst $Pd(QS)_2$ have used membranes from plants, microorganisms and mammals [7,12,13]. No studies have as yet been performed on fish membranes which, unlike the other groups, possess large proportions of long chain polyunsaturated fatty acids (PUFA's) such as 20:5ω3 and 22:6ω3. The abundance of PUFA's enables fish membranes to be progressively hydrogenated producing membranes with the full range of acyl group unsaturation. We show here that fish liver microsomes may be progressively and substantially hydrogenated by $Pd(QS)_2$ and we have defined the conditions giving optimal catalysis. Hydrogenation of the long chain C20 and C22 fatty acids was particularly rapid and complete hydrogenation was achieved without any fragmentation or loss of fatty acids. Finally, we show that hydrogenation was associated with large increases in bilayer lipid order and with the appearance of gel phase, as measured by fluorescence anisotropy using the membrane probe, 1,6-diphenyl-1,3,5-hexatriene (DPH).

2. Materials and methods

2.1. Materials

DPH (1,6-diphenyl-1,3,5-hexatriene) was ordered from Molecular Probes (Eugene, OR). $Pd(QS)_2$ was synthesised by F. Joó according to methods described elsewhere [11].

2.2. Animals

Trout (0.4–0.5 kg) were obtained from a commercial fish farm (Chirk Fisheries, Clywd, Wales) and kept at 12 ± 1°C for several weeks prior to the investigation. Carp (*Cyprinus carpio*, 0.3–0.7 kg) were obtained locally and maintained at 30 ± 1°C for several weeks. Fish were fed ad libitum once daily with standard feed pellets, sizes 110 for trout and 50 for carp (Trouw (UK), Longridge, Preston). The Antarctic fish species *Dissostichus mawsoni* were caught at McMurdo Sound, Antarctica, and kept at < -1°C.

2.3. Liver microsome preparation

Endoplasmic reticulum membranes were prepared from liver by modification of the method of Wodtke and Cossins [14]. Liver was minced, blended, homogenised by 8 passes of a glass-Teflon homogeniser in 5 vol (w/v) of 250 mM sucrose, 20 mM HEPES, pH 7.4 and centrifuged for 30 min at $10\,000 \times g$ and 4°C (J2-21 centrifuge, JA.20 rotor, Beckman). The resulting supernatant, to which was added 0.15 ml of CsCl for every 10 ml, was then centrifuged for 90 min at $120\,000 \times g$ and 4°C (Ultra Pro 80 centrifuge, T 865 titanium fixed angle rotor, Sorval). The upper microsomal pellet was resuspended in a small volume of buffer and then centrifuged at 14 000 rpm for 2 min to pellet any remaining glycogen.

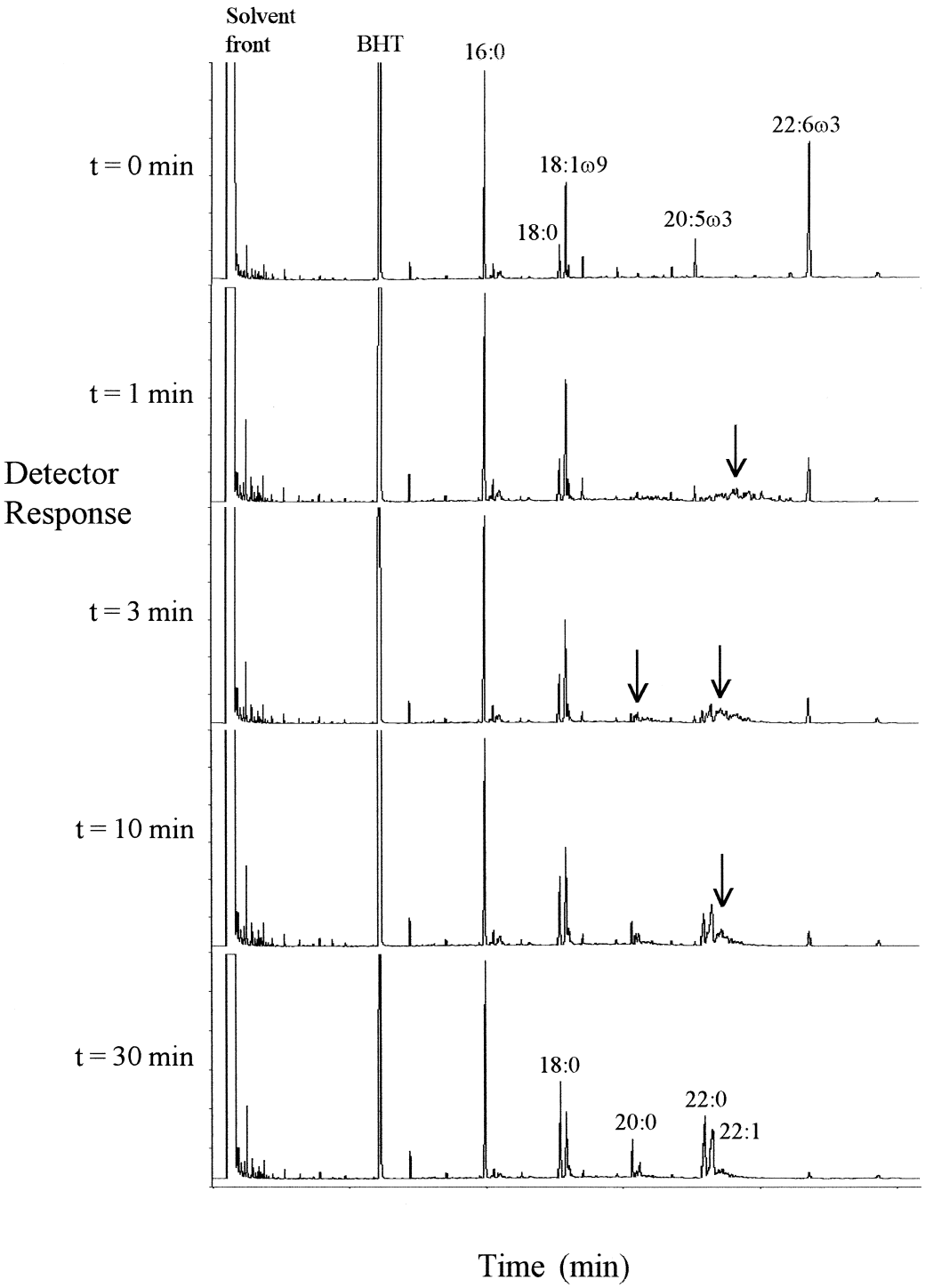

Fig. 1. The effects of catalytic hydrogenation on the fatty acid profile of trout liver microsomes. Gas chromatograms show fatty acid methyl esters from phosphatidylcholine, PC. t = time of hydrogenation. The $Pd(QS)_2$ concentration used was 0.2 mg/ml. Note the disappearance of 22:6ω3 and 20:5ω3 with hydrogenation and the appearance of a broad series of peaks of lower unsaturation (arrows). Further hydrogenation eventually leads to the predominance of the 20:0 and 22:0 saturates. The corresponding fatty acid data is shown in Table 1.

2.4. Hydrogenation procedure

Hydrogenation reactions were performed using glass, hydrogen-filled tonometers (Eschweiler, Keil, Germany) suspended in a temperature-controlled water bath. Unless otherwise stated, reactions were carried out at 25°C. Two tonometers were used for each reaction, one for catalyst pre-activation and the other for the reaction itself. Microsomal concentrations of 1.0 mg protein/ml and $Pd(QS)_2$ catalyst concentrations of 0.1 and 0.2 mg/ml were used.

For the reaction, a volume of degassed hydrogenation buffer (10 mM sodium phosphate, pH 6.5) and a homogeneous sample of liver microsomes were added to the reaction tonometer while degassed catalyst solution was added to the preactivation tonometer. When $Pd(QS)_2$ pretreatment was complete, as indicated by a red to yellow/brown colour change of the semi-hydrogenated, catalytically active complex [11], the catalyst was transferred to the reaction tonometer to initiate the reaction. At specific time intervals, samples of hydrogenated microsomes were withdrawn and pipetted into large glass test tubes where they were quickly shaken to re-oxidise the catalyst and stop the reaction.

2.5. Measurement of membrane physical properties

Membrane order was determined by steady-state fluorescence polarization using the probe DPH on a T-format fluorometer as described previously [15].

2.6. Lipid extraction and fatty acid analysis

Extraction of the total lipid fraction of the microsomal preparations and separation, isolation and transmethylation of the major phospholipid classes (phosphatidylcholine, PC, and phosphatidylethanolamine, PE) was performed as described previously [16]. The fatty acid methyl esters were analysed by gas-liquid chromatography (610 Series F.I.D. gas chromatograph, ATI Unicam, Cambridge) on a free fatty acid phase fused silica capillary column, 30 m × 0.25 mm (J and W Scientific, PhaseSep, Clwyd). The methyl esters were identified by comparing peak retention times to those of known standards whose identity had been confirmed by mass spectrometry.

3. Results

3.1. Effect of catalytic hydrogenation on membrane fatty acid composition

The effects of hydrogenation time upon the fatty acid composition of trout liver microsomes, PC fraction, are illustrated as a series of chromatograms in Fig. 1 with the corresponding calculated fatty acid composition in Table 1. Catalyst concentration was 0.2 mg/ml. The long chain PUFA's were particularly affected by hydrogenation. After just 1 min of hydrogenation, the percentage of 22:6ω3 in PC was reduced to one fifth (36.7–7.4%) and 22:5ω3 had

Table 1
Changes in the fatty acid composition of trout liver microsomes during hydrogenation

Fatty acid	Hydrogenation time (min)				
	Control	1	3	10	30
14:0	1.9	1.8	1.8	1.7	1.8
16:0	26.9	25.8	26.4	25.8	26.7
16:1ω7	1.9	1.8	1.6	1.4	0.9
18:0	3.6	4.6	6.1	8.4	11.1
18:1	16.0	16.5	15.6	13.8	10.4
18:2ω6	3.0	1.9	1.1	0.8	0.6
20:0	–	0.4	0.9	2.3	3.9
20:1	0.7	1.9	2.7	3.7	3.4
20:2ω6	0.3	–	–	–	–
20:x	–	6.2	5.1	4.3	1.9
20:4ω6	1.2	0.9	0.5	0.5	0.3
20:5ω3	6.1	1.3	0.8	0.4	0.1
22:0	–	0.5	2.1	6.1	13.4
22:1	–	1.7	6.5	12.7	16.0
22:x	–	27.2	24.0	15.6	8.7
22:5ω3	1.6	–	–	–	–
22:6ω3	36.7	7.4	4.8	2.3	0.9
% sat	32.4	33.1	37.3	44.5	56.9
% unsat	67.6	66.9	62.7	55.5	43.1
sat/unsat	0.48	0.50	0.60	0.80	1.32
% MUFA's	18.6	22.0	26.4	31.6	30.6
% PUFA's	49.0	44.9	36.2	24.0	12.5

Data are for phosphatidylcholine, PC, fatty acids following hydrogenation at a $Pd(QS)_2$ concentration of 0.2 mg/ml. Values are given as wt.% of the total fatty acid composition for each sample. The unidentifiable hydrogenated products of the C20 and C22 PUFA's are grouped as 20:x and 22:x respectively. The corresponding chromatograms are illustrated in Fig. 1.

disappeared. Continued hydrogenation led to a further reduction in 22:6ω3 until after 30 min it had almost completely disappeared. Associated with these decreases were concomitant increases in the products of PUFA hydrogenation. Because of the random positioning of hydrogenated double bonds, a large number of different acyl species with varying unsaturation and double bond positioning were formed, as evidenced from the appearance after 1 and 3 min of large numbers of small peaks (Fig. 1). Reliable separation and identification of these isomers was not possible and for quantitation they were grouped together as 20:*x* and 22:*x* fatty acids (Table 1).

Hydrogenation also resulted in the accumulation of trans-unsaturated fatty acid isomers from the cis form usually found in eukaryotic membranes. Fig. 2 shows the accumulation of trans-18:1ω9 following 60 min hydrogenation. These trans isomers may be formed from the hydrogenation of more unsaturated moieties or by cis/trans isomerization of existing 18:1ω9 acyl chains.

The C18 unsaturated fatty acids were hydrogenated at a much slower rate compared to the C20 and C22 chains; after 30 min 18:1 was reduced by only 35% whilst 22:6ω3 was reduced by 98%. However, the C18 unsaturates only occurred as di- and most predominantly monoenoics compared to the polyenoics of the longer chain fatty acids. Due to the stochastic nature of catalytic hydrogenation, the probability that a fatty acid will be hydrogenated is proportional to its number of unsaturated bonds. Previous studies have also observed a preferential saturation of polyunsaturated fatty acids compared to their monounsaturated counterparts [12,13].

Fig. 3 compares the rates of change in the individual fatty acid components for the PC and PE fractions. The hydrogenation of 22:6ω3 and C20 PUFA's was somewhat greater in PC than in PE (Fig. 3(a) and (b)) though the rates for C18 fatty acids were similar (Fig. 3(c)). Fig. 3(a) emphasises the extent to which 22:6ω3 was ultimately converted to its totally saturated form. After 30 min, 22:0 comprised 6.4% and

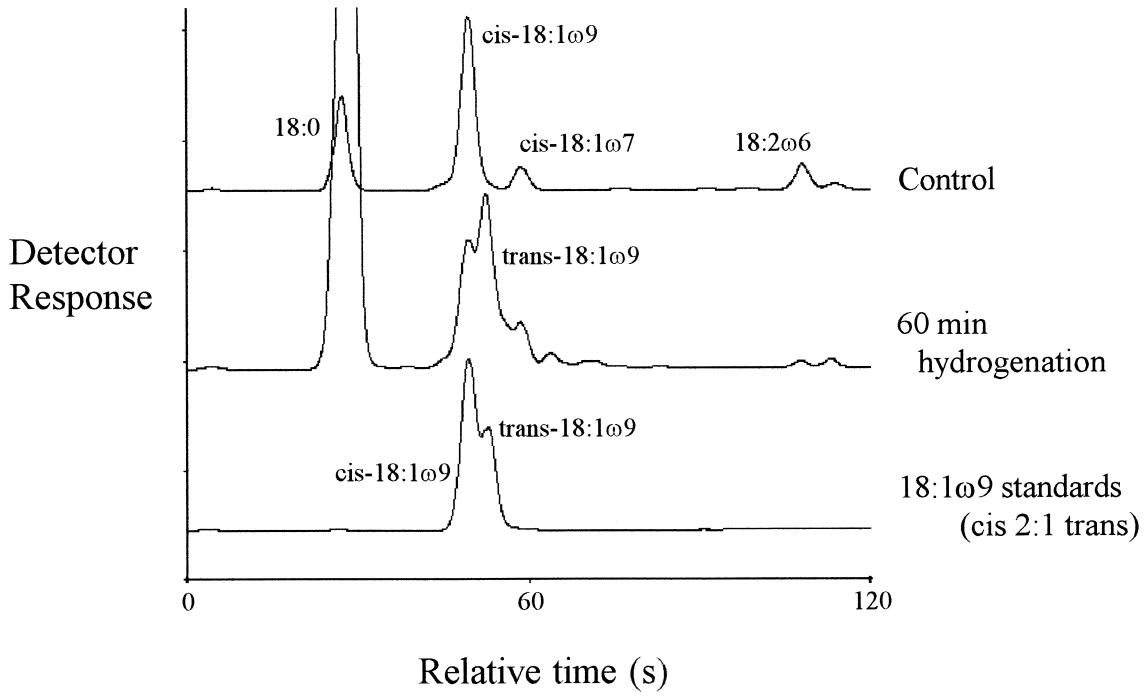

Fig. 2. The production of trans-fatty acid isomers following hydrogenation of trout liver microsomes. Gas chromatographs show the accumulation of trans-18:1ω9 after 60 min of hydrogenation from the all-cis control microsomes. cis and trans 18:1ω9 standards, at a ratio of 2:1, are shown for comparison.

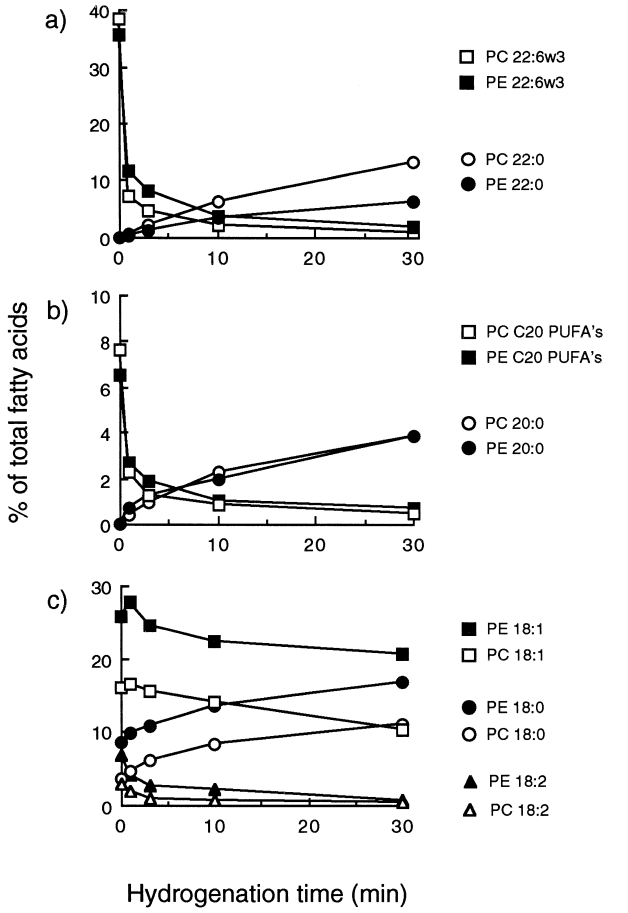

Fig. 3. Reductions in the proportions of C18, C20 and C22 unsaturated fatty acids and corresponding increases in their saturated forms. Hydrogenation results for phosphatidylcholine, PC, (open symbols) and phosphatidylethanolamine, PE, (filled symbols) from trout liver microsomes. (a) The reduction in 22:6ω3 and increases in the saturated 22:0. (b) The reduction in C20 PUFA's (20:2ω6, 20:4ω6 and 20:5ω3) and increases in 20:0. (c) The reduction of 18:2 and 18:1 unsaturates and corresponding increase in 18:0. Results are for a $Pd(QS)_2$ concentration of 0.2 mg/ml.

13.4% of the total fatty acids in PE and PC, respectively.

Changes in the fatty acid composition of trout microsomes were also analysed following hydrogenation at the lower catalyst concentration of 0.1 mg/ml (data not shown). These results showed the same trends discussed above, but at a reduced rate and extent of hydrogenation, suggesting that control over hydrogenation can be achieved by manipulation of the catalyst concentration. This effect is illustrated in Fig. 4 by plotting the increase in % saturated fatty acids for both PC and PE during hydrogenation. At the higher catalyst concentration, the percentage of saturated fatty acids after 30 min increased by 18.4% and 24.5% in PE and PC, respectively. As the proportions of 18:0 and 20:0 increased at equal rates in both lipids, this difference in saturation was attributed to the greater accumulation of 22:0 in PC (Fig. 3(a)).

An important control is to demonstrate that catalytic hydrogenation does not result in net losses of any particular group of fatty acids by fragmentation of hydrocarbon chains. Fig. 5(a) shows that this is not the case, since the relative proportions of the C16, C18, C20 and C22 fatty acids remained constant throughout the 30 min hydrogenation period. Fig. 5(b) shows that this was also true when the proportions of each chain length where calculated relative to an external standard. This discounts the unlikely probability of equal losses of fatty acids of different chain lengths. The external standard used was 18:3ω3, a fatty acid that did not occur naturally in these lipid samples and which was added in equal amounts to the samples after hydrogenation.

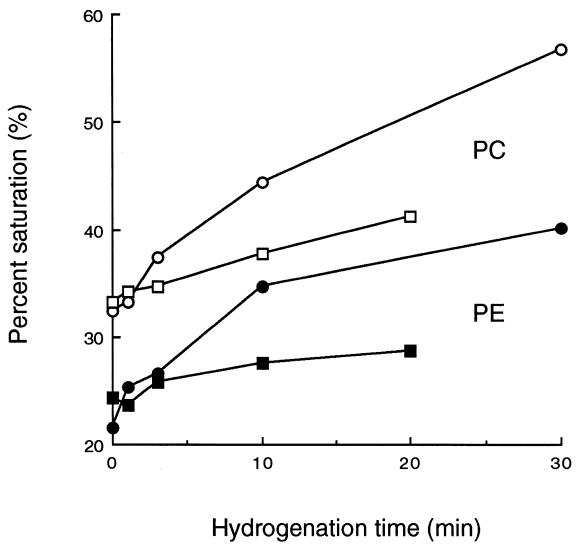

Fig. 4. The increase in saturated fatty acids of trout liver microsomes upon hydrogenation. Data are shown for phosphatidylcholine, PC (open symbols), and phosphatidylethanolamine, PE (filled symbols) at $Pd(QS)_2$ reaction concentrations of 0.1 mg/ml (squares) and 0.2 mg/ml (circles).

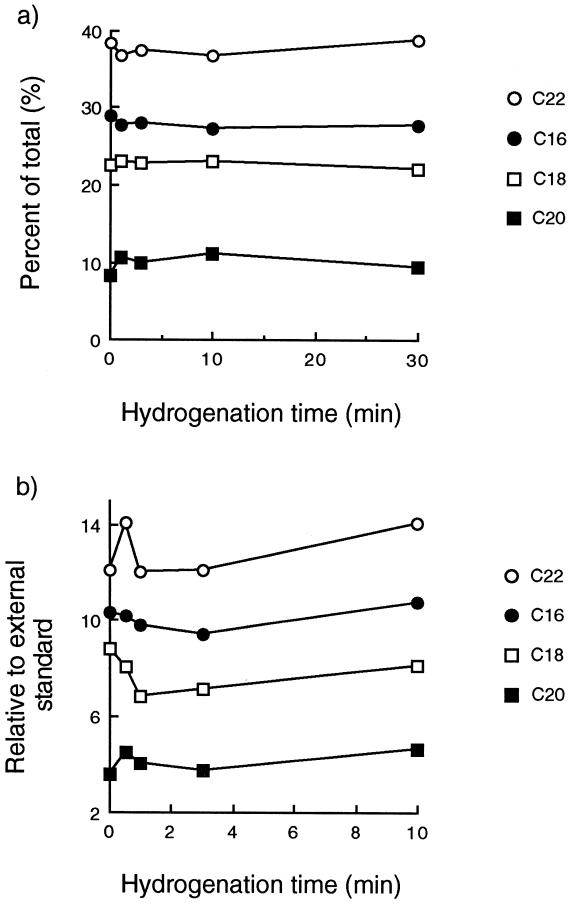

Fig. 5. Effect of hydrogenation on the relative proportions of C16, C18, C20 and C22 fatty acids within a sample. (a) Trout liver microsomal phosphatidylcholine, PC. (b) Total lipid fatty acids from carp liver microsomes relative to an external fatty acid standard (18:3ω3) added to the samples after hydrogenation. Both sets of data are for reactions at a $Pd(QS)_2$ catalyst concentration of 0.2 mg/ml.

3.2. Effect of catalytic hydrogenation on membrane physical properties

Despite the appreciable water solubility of $Pd(QS)_2$, removal of the catalyst from the membranes by simple washing proved impossible. Microsomes also remained labelled after repeated washing using bovine serum albumin (1%, w/w) and high KCl concentrations. Fluorescence anisotropy measurements were therefore made in the presence of the catalyst. We found that the presence of inactive $Pd(QS)_2$ within the microsomes affected the values of DPH anisotropy, an effect that increased linearly with catalyst concentration (data not shown). Modified Stern–Volmer plots were constructed (data not shown) and were consistent with a combined dynamic and static quenching of DPH by $Pd(QS)_2$ [17]. Preferential quenching of the longer lived photoactivated fluorophores would lead to loss of low anisotropy fluorescence and an increase in steady state values. However, at the catalyst concentrations employed in this work, the increase in anisotropy due to the inactive catalyst was small compared to the effects of hydrogenation itself (Fig. 8).

Hydrogenation of microsomal membranes was associated with large increases in DPH anisotropy. Fig. 6 illustrates this effect for liver microsomes obtained from a variety of species possessing different levels of polyunsaturated fatty acids at $Pd(QS)_2$ concentrations of 0.1 and 0.2 mg/ml. At the greater catalyst concentration, the DPH anisotropy increased very rapidly over the first ten minutes but with little change thereafter. At the lower catalyst concentration the increase in anisotropy occurred at a slower but more sustained rate.

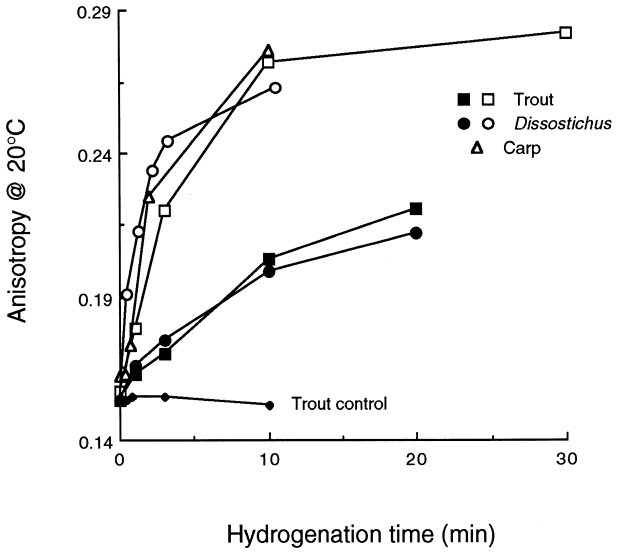

Fig. 6. Change in DPH fluorescence anisotropy during progressive hydrogenation of liver microsomes from different species. Trout (squares) and the Antarctic species *Dissostichus mawsoni* (circles) data are given for $Pd(QS)_2$ catalyst concentrations of 0.1 mg/ml (filled symbols) and 0.2 mg/ml (open symbols). Data are also supplied for carp (open triangles) microsome hydrogenation at a $Pd(QS)_2$ concentration of 0.2 mg/ml. The trout control was held under an N_2 atmosphere in the presence of 0.2 mg/ml of the catalyst.

3.3. Correlated changes in fatty acid saturation and membrane order

The relationship between fatty acid saturation and membrane physical properties is explored in Fig. 7. Percent saturation was used as an index of lipid composition since it is the first double bond that confers the greatest changes in physical properties [18–20]. We have separately plotted the curves calculated for PC and PE fatty acids. Membrane order was measured as DPH anisotropy at 25°C. Increasing saturation was clearly linked with increasing anisotropy, the relationship being linear over most of the range of saturation. At the highest saturations, however, further increases were associated with only small increases in anisotropy. This effect occurred at the longer periods of hydrogenation (>10 min) as shown in Fig. 6.

Fig. 8 illustrates the temperature dependence of DPH anisotropy for control and extensively hydrogenated membranes. Control membranes showed a progressive decrease in anisotropy with increase in temperature. Control membranes containing $Pd(QS)_2$ but not hydrogenated showed an identical temperature dependence, though anisotropies were slightly higher over the full temperature range. Membranes subjected to 10 min hydrogenation possessed much higher anisotropies, with values over the temperature range 3–30°C approximating those observed in artificial membranes in the gel condition [21]. On heating from 30 to 60°C, anisotropy decreased rapidly until a lower plateau was reached above 60°C. We interpret this as a phase transition with a gel state below 30°C, a liquid-crystalline state above 60°C and co-existing gel and liquid-crystalline microdomains at intermediate temperatures.

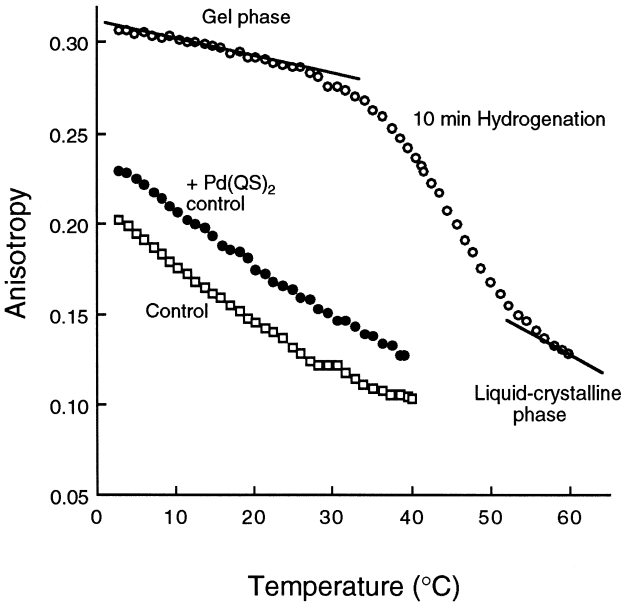

Fig. 8. Temperature-DPH fluorescence anisotropy plots for trout liver microsome preparations. Membrane samples shown are control (open squares), control containing inactive catalyst (filled circles) and 10 min hydrogenated samples (open circles). $Pd(QS)_2$ catalyst where present is at a concentration of 0.2 mg/ml.

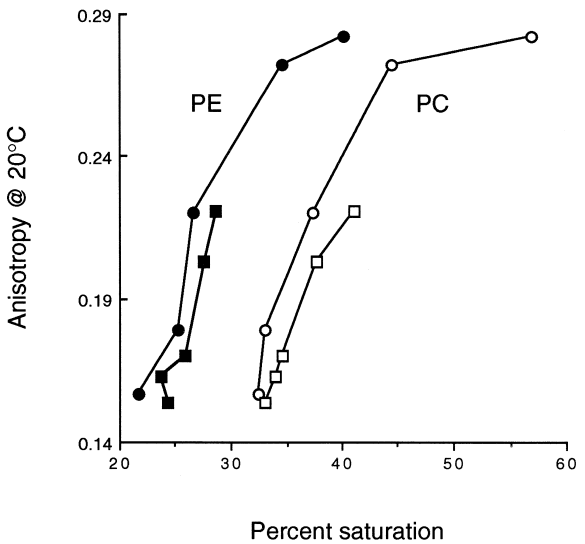

Fig. 7. The effect of increasing unsaturation on DPH fluorescence anisotropy values of trout liver microsomes. Results are given for phosphatidylcholine, PC, (open symbols) and phosphatidylethanolamine, PE, (filled symbols) following hydrogenation at $Pd(QS)_2$ catalyst concentrations of 0.1 mg/ml (squares) and 0.2 mg/ml (circles).

3.4. Temperature sensitivity of hydrogenation

Fig. 9(a) and (b) describe the interactions of temperature and time on the rate of hydrogenation, as measured by DPH anisotropy. Anisotropy increased more rapidly with increasing hydrogenation temperature, although anisotropy at 45°C was reduced, suggesting that hydrogenation was ineffective (Fig. 9(a)). The same data is replotted as a function of tempera-

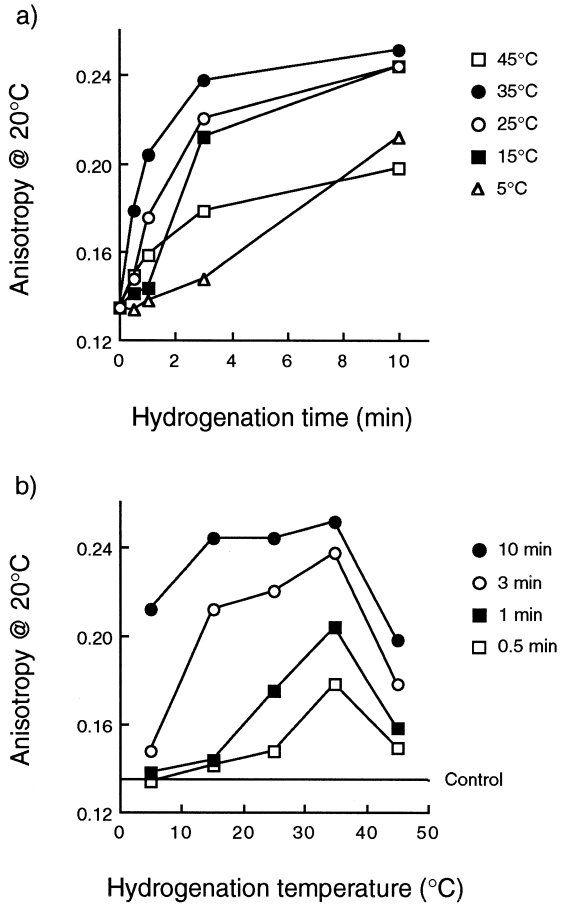

Fig. 9. Effect of reaction temperature on the rate and extent of hydrogenation. Results are for carp liver microsomes as measured by DPH fluorescence anisotropy at 20°C following hydrogenation at a $Pd(QS)_2$ catalyst concentration of 0.2 mg/ml.

ture in Fig. 9(b). This graph more clearly shows the rate-increasing effects of temperature and the reduction of rate at 45°C. At the lower hydrogenation temperatures, however, the initial slow rates of hydrogenation were followed by periods of rapid increase, for example between 3–10 min at 5°C and 1–3 min at 15°C (Fig. 9(b)).

4. Discussion

$Pd(QS)_2$ has proved to be a very effective catalyst for the hydrogenation of animal membranes and we show here that this is also true of PUFA-rich membranes from trout. Hydrogenation proceeds rapidly with an early hydrogenation of polyunsaturated fatty acids, and a slower, more sustained hydrogenation of monounsaturated fatty acids.

Comparison of the two major phospholipid classes revealed a preferential hydrogenation of C20 and C22 PUFA's and a greater accumulation of 22:0 in PC compared with PE, a difference that has been previously observed in model membranes [5]. Although there may be some inherent differences in the reactivity of the two phospholipid classes due to their different headgroups, this selectivity may be due to the differences in accessibility of the catalyst to each of the lipids [5]. Lipids lying deep within multibilayer systems or on the inner leaflet of a single bilayer would be less accessible. Phospholipids are asymmetrically distributed in biomembranes with PE existing predominantly on the inner leaflet [22]. On the other hand, accessibility of the catalyst to fatty acid substrates may be related to membrane order, both before and during hydrogenation [8,23].

We demonstrate a close correlation during progressive hydrogenation between % saturation of the major phospholipids and membrane order as measured by DPH anisotropy. Firstly, this shows that, despite reservations about its suitability for monitoring changes in chain length or degree of unsaturation of membrane lipids [24], the motional properties of DPH incorporated into a biological membrane are highly sensitive to variations in lipid saturation and this probe samples a predominantly lipid environment. Secondly, it demonstrates the sensitivity of the physical structure of a biological membrane containing all the normal membrane components to variations in fatty acid saturation, having effectively excluded variations in other membrane components. This lends strong support to the claimed causal link between altered fatty acid saturation and changes in membrane order during thermal acclimation [25]. The correlation was strong and linear when the membranes were in the non-gel state and when lipid composition was expressed as % saturated fatty acids.

Unfortunately, the enormous complexity of the partially hydrogenated fatty acid isomers prevents their structural identification and it is not possible to separate the physical effects of early hydrogenation, when long chain PUFA's such as 20:5ω3 and 22:6ω3 are being partially hydrogenated, from those of extended hydrogenation when C18 monounsaturated fatty acids are being hydrogenated. It was therefore

not possible to calculate the equivalent unsaturation index of the hydrogenated microsomes or to define the relationship of physical structure with degree of polyunsaturation. In any case, bilayer physical properties appear to be more closely related to the proportion of saturated and unsaturated fatty acids rather than to the number of unsaturation bonds [20], therefore structure should be more dependent on the hydrogenation of monounsaturated and diunsaturated fatty acids than on the conversion of hexaenes to pentaenes or tetraenes.

Extended hydrogenation (>10 min) leads to a reduced but continuing rate of hydrogenation whilst DPH anisotropy shows no further change. This might indicate that some hydrogenation events (i.e. on diunsaturated and monounsaturated species) have no physical effect upon the bilayer. However, we show that these heavily hydrogenated microsomes have DPH anisotropies that are characteristic of gel phase bilayers. Furthermore, we show that with increasing temperatures these membranes display the characteristic sigmoidal anisotropy curve for a phase transition with onset at 30°C and a completion at approximately 60°C. Thus, the apparent uncoupling between saturation and physical structure noted in Fig. 7 is due to the occurrence of the gel state at the temperature used for measurement of DPH anisotropy; the gel state membrane is at the point of maximal order such that increased saturation would have no additional effect. Increasing the temperature for anisotropy determination to a point within the melting profile would allow the close link between saturation and physical order to be extended to longer hydrogenation times.

The catalytically active, semi-hydrogenated complex of $Pd(QS)_2$ is a radical anion and its hydrogenation of C=C bonds in homogeneous aqueous solutions proceeds at a rapid rate that is practically independent of temperature; in the case of crotonic acid hydrogenation, an overall activation energy of 16.4 kJ/mol has been established [26]. It is unclear, therefore, why a temperature-dependent reaction rate is observed in Fig. 9(a) and (b). In contrast to homogeneous solutions of one substrate, however, several factors may contribute to an overall temperature dependence. These include the spatially uneven distribution of various lipids, the temperature-dependent membrane lipid order, transient formation of many different lipids with varying degrees of unsaturation, significant cis/trans isomerization of the unsaturated fatty acyl moieties with concomitant rigidification of the membranes and, finally, the hydrogen activation by the catalyst itself. Nevertheless, independent of the time course of hydrogenation, a substantial saturation could be achieved in 10 min at all the investigated temperatures.

During this study we have found it difficult to remove the catalyst from liver microsomes, the membranes remaining distinctly coloured despite extensive washing in the presence of bovine serum albumin and high concentrations of KCl. It is thought that the negatively charged sulphonate groups of such catalysts may bind to membrane-bound and other proteins [27], thus inhibiting removal. Moreover, binding of the catalyst, without hydrogenation, was sufficient to inhibit a variety of membrane-associated enzymes such as the (Na–K)ATPase and the NADPH: cytochrome c reductase (J.A. Logue, unpublished data), and affect survival of cultured cells [9], (J.A. Logue, and E. Fodor, unpublished data).

On the other hand, in their extensive work with $Pd(QS)_2$, Vigh and co-workers have been able to remove successfully the catalyst from a variety of plant membrane systems [28], intact algal cells [29] and also mammalian systems [13]. They have also reported many instances of no detrimental effect of the inactive catalyst on membrane function [13,30–32]. More importantly, mammalian and cyanobacterial cells remain viable after incubation with the catalyst and even after hydrogenation itself. There is evidently some difference in binding characteristics of the catalyst between different kinds of membrane which is presumably due to their divergent protein or lipid compositions. Vigh and colleagues have more recently developed a series of catalysts in which the metal is either in the form of a protected colloid [33] or deposited on the surface of water-insoluble polymer compounds [34]. These catalysts can be removed more completely from cell suspensions and without damage to cells and may prove useful in polyunsaturated membranes.

Acknowledgements

We acknowledge BBSRC for a studentship for JAL.

References

[1] R.B. Gennis, Biomembranes: Molecular Structure and Function, Springer, New York, 1989.
[2] N. Murata, O. Ishizaki-Nishizawa, S. Higashi, H. Hayashi, Y. Tasaka, I. Nishida, Nature 356 (1992) 710–713.
[3] L. Carratu, S. Franceschelli, C.L. Pardini, G.S. Kobayashi, I. Horvath, L. Vigh, B. Maresca, Proc. Natl. Acad. Sci. U.S.A. 93 (1996) 3870–3875.
[4] A.V. Bulatov, E.N. Izakovich, L.N. Karklin, M.L. Khidekel, Izv. Akad. Nauk. SSSR, Ser. Khim. 9 (1981) 2032–2035.
[5] L. Vigh, I. Horvath, F. Joó, G.A. Thompson, Biochim. Biophys. Acta 921 (1987) 167–174.
[6] I. Horvath, Z. Torok, L. Vigh, M. Kates, Biochim. Biophys. Acta 1085 (1991) 126–130.
[7] M. Schlame, L. Horvath, L. Vigh, Biochem. J. 265 (1990) 79–85.
[8] L. Vigh, F. Joó, FEBS Lett. 162 (1983) 423–427.
[9] Y. Pak, F. Joó, L. Vigh, A. Katho, G.J. Thompson, Biochim. Biophys. Acta 1023 (1990) 230–238.
[10] B. Szalontai, M. Droppa, L. Vigh, F. Joó, G. Horvath, Photochem. Photobiol. 10 (1986) 233–240.
[11] F. Joó, N. Balogh, L.I. Horvath, G. Filep, I. Horvath, L. Vigh, Anal. Biochem. 194 (1991) 34–40.
[12] S. Benko, H. Hilkmann, L. Vigh, B.W.J. van, Biochim. Biophys. Acta 896 (1987) 129–135.
[13] M. Schlame, I. Horvath, Z. Toeroek, L.I. Horvath, L. Vigh, Biochim. Biophys. Acta 1045 (1990) 1–8.
[14] E. Wodtke, A.R. Cossins, Biochim. Biophys. Acta 1064 (1991) 343–350.
[15] A.R. Cossins, A.G. Macdonald, Biochim. Biophys. Acta 860 (1986) 325–335.
[16] J.A.C. Lee, A.R. Cossins, Biochim. Biophys. Acta 1026 (1990) 195–203.
[17] J.R. Lakowicz, Principles of Fluorescence Spectroscopy, Plenum Press, New York, 1983.
[18] K.P. Coolbear, C.B. Berde, K.M.W. Keough, Biochemistry 22 (1983) 1466–1473.
[19] C. Stubbs, A.D. Smith, Biochim. Biophys. Acta 779 (1984) 89–137.
[20] A.R. Cossins, J.A.C. Lee, in: R. Gilles (Ed.), Circulation, Respiration and Metabolism, Springer, Berlin, 1985, pp. 543–552.
[21] T. Parasassi, F. Conti, M. Glaser, E. Gratton, J. Biol. Chem. 259 (1984) 14011–14017.
[22] R.J. Hitzemann, R.A. Harris, H.H. Loh, in: M. Shinitzky (Ed.), Physiology of Membrane Fluidity, vol. II, CRC Press,Boca Raton, FL, 1984, pp. 109–126.
[23] C. Vigo, F.M. Goni, P.J. Quinn, D. Chapman, Biochim. Biophys. Acta 508 (1978) 1–14.
[24] R.N. McElhaney, in: A.R. Cossins (Ed.), Temperature Adaptation of Biological Membranes, Portland Press, London, 1994, pp. 31–48.
[25] A.R. Cossins, in: A.R. Cossins (Ed.), Temperature Adaptation of Biological Membranes, Portland Press, London, 1994, pp. 63–76.
[26] F. Joó, G. Filep, L. Vigh, Proceedings of 7th Int. Symp. Homogeneous Catal., Lyon, 1990, p. 147.
[27] P.J. Quinn, F. Joó, L. Vigh, Prog. Biophys. Mol. Biol. 53 (1989) 71–103.
[28] G. Horvath, M. Droppa, T. Szito, L.A. Mustardy, L.I. Horvath, L. Vigh, Biochim. Biophys. Acta 849 (1986) 325–336.
[29] L. Vigh, I. Horvath, G.A.J. Thompson, Biochim. Biophys. Acta 937 (1988) 42–50.
[30] C. Demandre, L. Vigh, A.M. Justin, A. Jolliot, C. Wolf, P. Mazliak, Plant Science 44 (1986) 13–21.
[31] I. Horvath, L. Vigh, T. Pali, G.A.J. Thompson, Biochim. Biophys. Acta 1002 (1989) 409–412.
[32] L. Vigh, F. Joó, M. Droppa, L. Horvath, G. Horvath, Eur. J. Biochem. 147 (1985) 477–481.
[33] L. Nadasdi, I. Horvath, L. Vigh, S. Benko, F. Joó, React. Kin. Catal. Lett. 59 (1996) 227–233.
[34] F. Joó, F. Chevy, O. Colard, C. Wolf, Biochim. Biophys. Acta 1149 (1993) 231–240.